Ocean Science Journal, Vol. 41 No. 2, 97-104(2006)

Article

Ocean Science Journal

http://osj.kordi.re.kr

Method of Integrating Landsat-5 and Landsat-7 Data to Retrieve Sea Surface Temperature in Coastal Waters on the Basis of Local Empirical Algorithm

Qianguo Xing, Chu-qun Chen*, and Ping Shi

LED, South China Sea Institute of Oceanography, Chinese Academy of Science, 164# West Xin Gang Road, Guangzhou 510301, China

Received 17 March 2006; Revised 7 June 2006; Accepted 23 June 2006

Abstract – A useful radiance-converting method was developed to convert the Landsat-7 ETM+thermal-infrared (TIR) band's radiance ($L_{\lambda,L7/ETM+}$) to that of Landsat-5 TM TIR ($L_{\lambda,L5/TM}$) as: $L_{\lambda,L5/TM}=0.9699\times L_{\lambda,L7/ETM+}+0.1074$ ($R^2=1$). In addition, based on the radiance-converting equation and the linear relation between digital number (DN) and at-satellite radiance, a DN-converting equation can be established to convert DN value of the TIR band between Landsat-5 and Landsat-7. Via this method, it is easy to integrate Landsat-5 and Landsat-7 TIR data to retrieve the sea surface temperature (SST) in coastal waters on the basis of local empirical algorithms in which the radiance or DN of Lansat-5 and 7 TIR band is usually the only input independent variable. The method was employed in a local empirical algorithm in Daya Bay, China, to detect the thermal pollution of cooling water discharge from the Daya Bay nuclear power station (DNPS). This work demonstrates that radiance conversion is an effective approach to integration of Landsat-5 and Landsat-7 data in the process of a SST retrieval which is based on local empirical algorithms.

Key words – remote sensing, sea surface temperature, Landsat, coastal waters

1. Introduction

Thermal infrared (TIR) remote sensing technique is a useful approach to monitor the change of water temperature (Schott 1982; Schott *et al.* 2001; Ritchie and Cooper 2001). Advanced Very High Resolution Radiometer (AVHRR) and Moderate Resolution Imaging Spectroradiometer (MODIS) TIR data are widely used in current global sea surface temperature (SST) retrieval, but their poor spatial resolution (1.1 km) may not be adequate for detecting thermal plumes in morphologically complex coastal waters (Ahn *et al.* 2006; Tang *et al.* 2003; Thomas *et al.* 2002), *e.g.* the Daya Bay extends only about 10 kilometers in the west-east direction, and there are many islands in the central bay; if AVHRR data are used, only a few pure pixels can be found on the image and it is hard to obtain detailed SST distribution pattern. TIR Bands of Landsat-5 Thematic Mapper (TM), Landsat-7 Enhanced Thematic Mapper plus (ETM+), and Advanced Spaceborne Thermal Emission and Reflectance Radiometer (ASTER), have very higher resolutions of 120 m, 60 m and 90 m, respectively, and they are widely used for the retrieval of sea surface temperature (SST) in coastal waters (Gibbons *et al.* 1989; Chen *et al.* 2003; Mustard *et al.* 1999; Suga *et al.* 2003).

Based on the fact that the atmosphere has different effects on different TIR bands of AVHRR and MODIS, a split-window algorithm is widely used in SST retrieval with AVHRR and MODIS data, and it can remove the atmospheric effects to a satisfying extent, especially for open sea. For TM and ETM+, both of them have only one TIR band, so the split-window algorithm is not applicable. The difficulty of atmospheric correction limits the use of TM/ETM+ TIR bands in coastal and inland waters (Ritchie and Cooper 2001; Schott *et al.* 2001). To overcome this limit, many researchers (Chen *et al.* 2003; Suga *et al.* 2003; Thomas *et al.* 2002) have developed local empirical algorithms to retrieve SST on the basis of the radiance or DN value of Ladnsat-5 TM and Landsat-7 ETM+ TIR data,

*Corresponding author. E-mail: cqchen@scsio.ac.cn

and no atmospheric correction work needs to be done. However, these empirical algorithms based on Landsat-5 TM and Landsat-7 ETM+ are exclusive, and can not be applicable to each other, which makes it difficult to use the two different sources of data.

This paper will introduce a method of integrating Landsat-5 and Landsat-7 TIR data to retrieve sea surface temperature in coastal waters.

2. Materials and Methods

Testing area and Landsat TIR data

Daya Bay lies to the eastern side of the Pearl River estuary (114°30'~114°50'E, 22°30'~22°51'N), close to Hong Kong, Dapeng Bay and Honghai Bay, covering about 600 km^2, and it is a typical semi-enclosed subtropical bay (Fig. 1) (Xu 1989). It is also an important protected area for marine fisheries resources in Guangdong province. In the last 20 years, the local economy has experienced great progress, and accordingly the energy industry increased rapidly. Daya Bay Nuclear Power Station (DNPS, 1800 MW) has been in operation since 1994, Ling'ao Nuclear Power Station (LNPS, 4000 MW) near DNPS is under construction, and another power plant (8000 MW) is planned to be set up on the east coast of Daya Bay. The thermal pollution of cooling water discharged from these power stations will lead to potential habitat damage of local marine organisms, *e.g.* fish and coral.

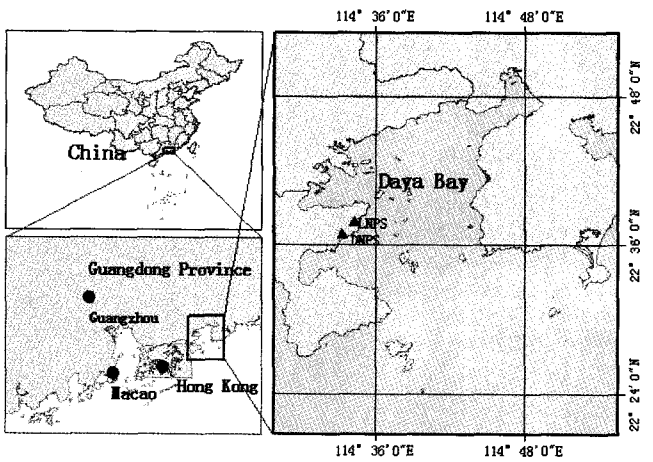

Fig. 1. Location of Daya Bay.

Daya Bay Nuclear Power Station (DNPS) was put into use officially in 1994, and in order to investigate the SST change before and after the operation of DNPS, we selected three Landsat images acquired over Daya Bay in 1991, 2001, and 2004 (Table 1). Landsat-5 and Landsat-7 pass over Daya Bay at a local time of about 10:00 AM, and they have very high spatial resolutions of thermal bands, i.e., 120 m and 60 m, respectively, which make them more useful in retrieving SST in coastal waters.

Methods of SST retrieval

Method based on Planck's radiance function

The basic steps of retrieving ground surface temperature by Landsat TIR data are as follows:

First, convert digital number (DN, unit less) to at-satellite radiance (L_λ, W m^{-2} sr^{-1} μm^{-1}) as a linear relation between them:

$$L_\lambda = \text{gain} \times \text{DN} + \text{offset} \quad (1)$$

where the value of gain and offset can be found or calculated from parameters provided in the header file of data (Landsat Project Science Office 2006).

Second, convert the at-satellite radiance to at-satellite brightness temperature as Eq. 2, which is an approximation to Planck's radiance function (Qin *et al.* 2001).

$$T_B = T_{sensor} = \frac{K_2}{\ln(k_1 / L_\lambda + 1)} \quad (2)$$

where k_1 and K_2 are calibration constants as in Table 2 (Chander and Markham 2003; Landsat Project Science Office 2006).

If no atmospheric effects are included, at-satellite radiance (or TOA radiance) can be regarded as ground surface radiance, and the sea surface brightness temperature (T_B, K) will be equal to at-satellite brightness temperature (T_{sensor}, K). In a simple way, T_B can be regarded as an approximation

Table 1. The Landsat TIR data acquired over Daya Bay

Date of Acquisition (month-day-year)	Platform/sensor	Ground resolution, m	Wavelength, μm
10-09-1991	Landsat-5/TM	120	10.40-12.50
12-31-2001	Landsat-7/ETM+	60	10.40-12.50
02-15-2004	Landsat-5/TM	120	10.40-12.50

Table 2. TM/ ETM+ Thermal Band Calibration Constants

Sensor	Calibration Constants	
	k_1, W m^{-2} sr^{-1} m^{-1}	K_2, K
Landsat-5 TM	607.76	1260.56
Landsat-7 ETM+	666.09	1282.71

to actual SST (Ahn *et al.* 2006).

Method based on local empirical algorithm

In most cases, the atmospheric effects cannot be ignored, especially for coastal waters, *e.g.* Daya Bay where the water vapor concentration is considerably high in the air column. Water vapor can absorb thermal infrared radiation greatly, and the thermal radiation from ground surface will be reduced before reaching TIR sensors on Landsat. Therefore, if Planck's radiance function is adopted in SST retrieval, atmospheric correction should be done (Qin *et al.* 2001; Xing *et al.* 2006). But, because it is usually hard to find an effective atmospheric correction method, many researchers prefer establishing local empirical algorithms of SST retrieval in which the radiance or DN of TIR band is usually the only input independent variable (Chen *et al.* 2003; Suga *et al.* 2003; Thomas *et al.* 2002).

Chen *et al.* (2003) developed a very useful local algorithm called summer-winter united algorithm for the SST retrieval in Daya Bay. This algorithm (Eq. 3) was established as the correlation relationship between the radiance and in-situ SST data collected under summer and winter weather conditions, and it is applicable to Landsat-5 TM TIR data. Its absolute error and relative error are 0.03±0.51°C and -0.22±2.46%, respectively, which can meet the request of SST retrieval accuracy, so it will be employed in our work.

$$SST=149.55\times L_{\lambda}-98.703,\ (R^2=0.9943) \quad (3)$$

where the units of SST and L_{λ} are and W cm^{-2} sr^{-1} μm^{-1}, respectively.

Converting the TIR radiance between Landsat-7 and Landsat-5

Although the TIR bands of Lansat-5 and Landsat-7 have a same nominal bandwidth of 10.4-12.5 μm and similar orbit characteristics (Vogelmann *et al.* 2001), the radiances recorded by them are different when a same target was mapped concurrently. This is because their relative spectral response (RSR) characteristics are different from each other (Landsat Project Science Office, 2006) (see Fig. 2). The different RSR characteristics also explain why different calibration constants are used in Eq. 2 to calculate at-satellite temperature. Eq. 3 was established based on Landsat-5 TM TIR data, so it is not applicable to Landsat-7 TIR data, and the Landsat-7 ETM+ TIR radiance ($L_{\lambda,L7/ETM+}$) should be converted to corresponding Landsat-5 TM TIR radiance ($L_{\lambda,L5/TM}$) before using Eq. 3 to retrieve SST in Daya Bay.

In the research of Vogelmann *et al.* (2001) and Chen *et al.* (2004), in order to take advantages of the superior radiometric calibration of ETM+, the Landsat-5 TM DN (DN5) was firstly converted to ETM+ DN (DN7) as: DN7 = (DN5 × slope) + intercept, where slope and intercept were

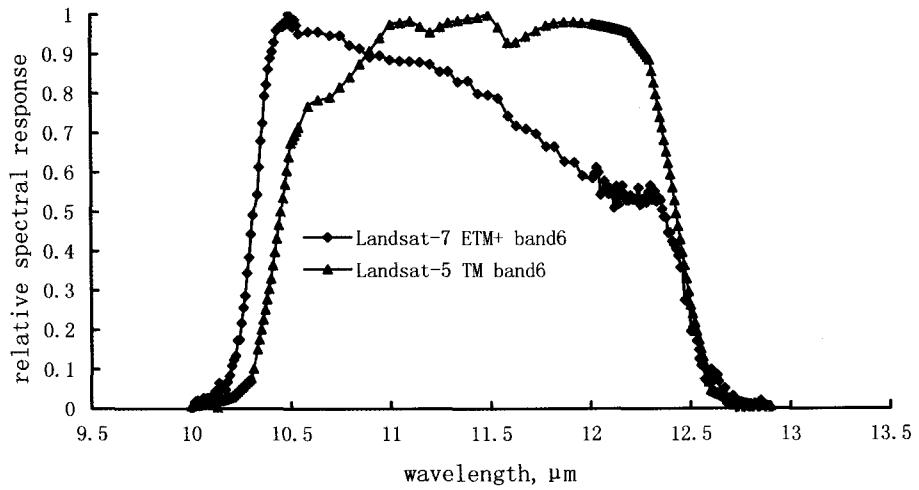

Fig. 2. The relative spectral response profiles of Landsat-5 TM and Landsat-7 ETM+ TIR band.

obtained by statistical analysis with the DNs of pixel pairs from TM and ETM+ images which were mapping the same targets coincidently. But their work did not include the TIR bands.

In order to convert $L_{\lambda,L7/ETM+}$ to $L_{\lambda,L5/TM}$, we can presume an ideal situation where a same ground target is coincidently mapped by Landsat-5 and Landsat-7 at a same spatial location on orbit, then T_{sensor} should be the same to each other for the same target on the two images because T_{sensor} is only up to the thermal characteristics of the ground target and the air above it, no matter how different the radiance is recorded by TM and ETM+. Thus, from Eq. 2 and Table 2, we can get the following equation to describe the relation between the radiance recorded by Landsat-5 TM and that by Landsat-7 ETM+:

$$\frac{1260.56}{\ln(607.76/L_{\lambda,L5/TM}+1)} = \frac{1282.71}{\ln(666.09/L_{\lambda,L7/ETM+}+1)} \quad (4)$$

In Eq. 1, the gain and offset may vary with different data processing systems, but the scope of L_λ will not change too much. For the Landsat-5 TM TIR Data processed by U.S. NLAPS (Chander and Markham, 2003), Eq. 1 can be set as: L_λ=(0.055158×DN)+1.2378, and L_e ranges in the scope of 1.29~15.30 W m^{-2} sr^{-1} μm^{-1} because DN value ranges from 1 to 255. In the scope of 1~16 W m^{-2} sr^{-1} μm^{-1}, we investigated the relationship between $L_{\lambda,L7/ETM+}$ and $L_{\lambda,L5/TM}$, and found that they had a very good linear relationship (Fig. 3). The relationship can be described as Eq. 5 which is much simpler than Eq. 4, and it will be used to convert $L_{\lambda,L7/ETM+}$ to $L_{\lambda,L5/TM}$ after we calculate $L_{\lambda,L7/ETM+}$ by the equation of L_λ=(0.0370588×DN)+3.2 (for the TIR data with high gains) (Weng *et al.* 2004; Landsat Project Science Office 2006).

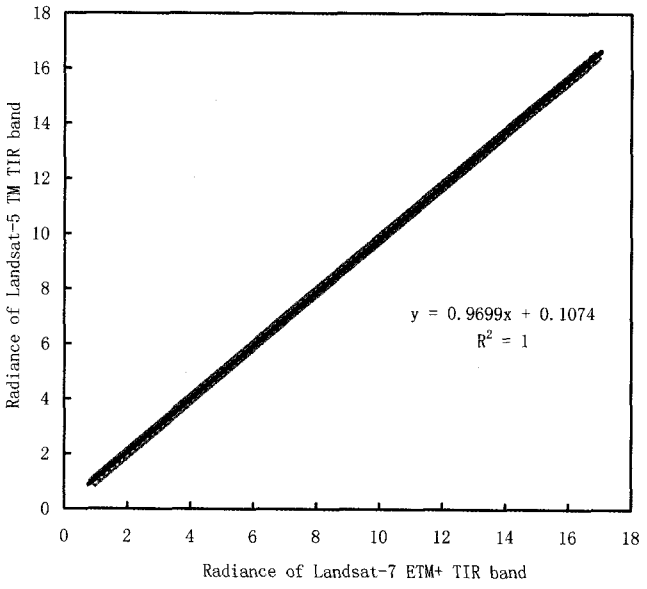

Fig. 3. The relationship of radiances between Landsat-5 TM and Landsat-7 ETM+ TIR band, W m^{-2} sr^{-1} μm^{-1}.

$$L_{\lambda,L5/TM}=0.9699\times L_{\lambda,L7/ETM+}+0.1074,\ (R^2=1) \quad (5)$$

Vice versa, the Eq. 5 can be used to convert $L_{\lambda,L5/TM}$ to $L_{\lambda,L7/ETM+}$ also. If necessary, a DN-converting equation between Landsat-5 and Landsat-7 can also be deduced according to Eq. 5 and Eq. 1.

Image processing and SST retrieval

Image processing must be done before SST retrieval, and the whole process is as shown in Fig. 4: Firstly, register all the collected images to a same map, and keep them matched with each other geographically; secondly, find the targeted area and detruncate the images; thirdly, divide the whole image into water and land, and mask the land part; fourthly, convert DN to radiance for the water part; if the TIR image is acquired by Landsat-7 ETM+,

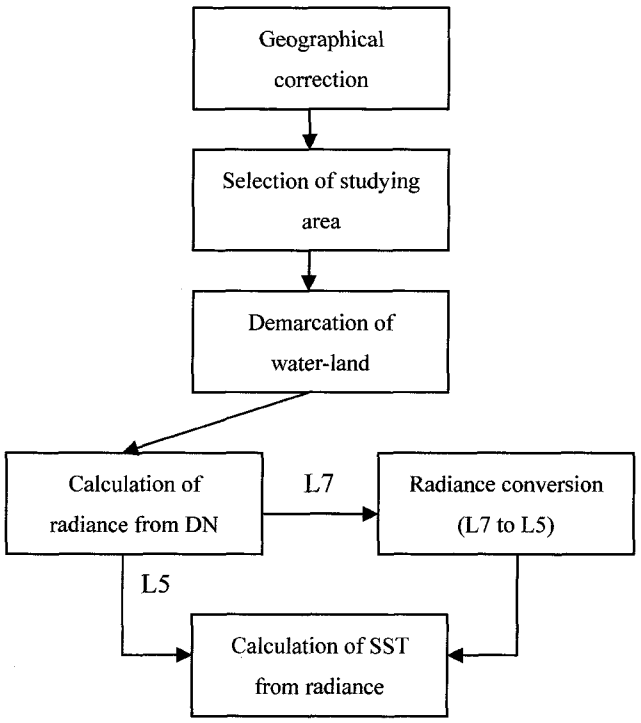

Fig. 4. The diagram of image processing and SST retrieval (L7---Landsat-7, L5—Landsat-5).

the radiance will be further converted to that of Landsat-5 TM; and lastly, retrieve SST on the basis of radiance. All the process can be accomplished with the software of ENVI 4.0 and IDL 6.0.

3. Results and Discussion

The method of integrating Landsat data based on local algorithm

When the Landsat-7 ETM+ data are used to retrieve SST based on the local algorithm developed by Chen *et al.* (2003) for Daya Bay, the steps are as below:

Step 1, calculate radiance with Eq. 1;

Step 2, convert Landsat-7 ETM+ radiance to Landsat-5 TM radiance with Eq. 5, and

Step 3, retrieve SST with Eq. 3.

If Landsat-7 ETM+ TIR data are used in Eq. 5 without step 2, we find that it will underestimate the actual SST by 1.3°C to 2.7°C when at-satellite radiance ranges from 7 W m^{-2} sr^{-1} μm^{-1} to 10 W m^{-2} sr^{-1} μm^{-1} (see Fig. 5). Thus, step 2 cannot be omitted for Landsat-7 ETM+ TIR data while only step 1 and step 3 are needed for Landsat-5 TM TIR data.

With the three steps, Landsat-5 and Landsat-7 TIR data can be integrated to monitor the thermal pollution of cooling water discharged from the DNPS. In this research, Eq. 3 is a local empirical algorithm for Daya Bay, and it is based on TIR radiance of Landsat-5 TM; when it comes to other situations where Eq. 3 changes with geo-location, source of data (Landsat-7 or Landsat-5), input variable (radiance or DN value), this integrating method also can be applied with a slight modification.

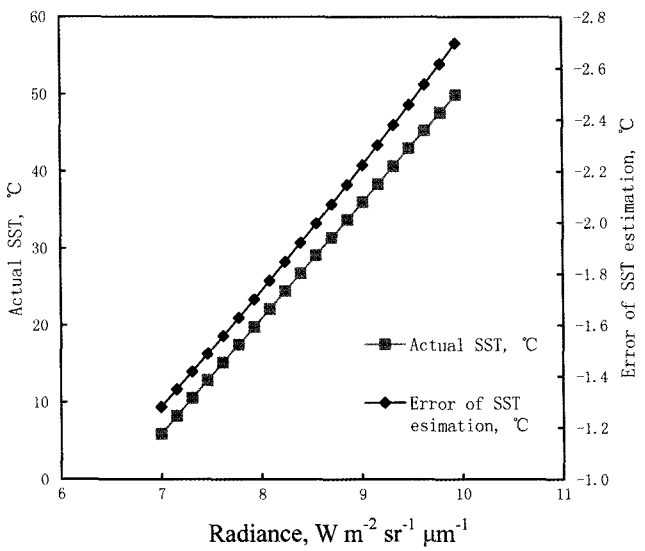

Fig. 5. The error of SST estimated with ETM+ radiance directly used in the local algorithm for TM data.

Validation

Prior to the actual implementation of this approach, validation work was conducted to test the results when Landsat-7 ETM+ TIR radiance was converted to Landsat-5 TM TIR data.

It may be an ideal way to do validation by obtaining the *in-situ* SST data simultaneously with the overpass of Landsat-7. But, due to no *in-situ* data available, MODIS terra data were processed to SST data with the software of SeaDAS 4.6 in which a split window algorithm was employed, and the SST was set as reference for comparison. Xing *et al.* (2006) in earlier work has proved that the retrieved SST from MODIS terra data matches the actual SST very well in Daya Bay, so it is reasonable to use this validation method.

Based on the fact that the spatial resolutions of ETM+ and MODIS TIR bands are 60 m and 1.1 km, respectively, the ETM+ SST result was re-sampled to the mean value of a window of 17×17 pixels, then 26 sampling points was set on MODIS terra image to match the corresponding points on Landsat-7 ETM+ image. The SST results from the two kinds of remote sensing dataset showed that the SST result of ETM+ was lower than that of MODIS by 0.93±0.47°C (Fig. 6), and that there was a good linear correlation relationship between them (see Fig. 7). The gap of 0.93°C can be mitigated if it is considered that the time of MODIS Terra's overpass was about 1h later than that of Landsat-7 ETM+, and that the actual SST will increase gradually in the morning due to solar radiation. The result of this local algorithm is even better than that of other algorithms (Xing *et al.* 2006).

This validation demonstrates that converting the TIR radiance from Landsat-7 ETM+ to Landsat-5 TM is an effective way to integrate the data from the two different platforms in SST retrieval on the basis of local empirical algorithm.

Thermal pollution detection in Daya Bay

Due to the possible thermal pollution, thermal effluent from power plant is the focus of many researchers' work, and remote sensing techniques played an important role

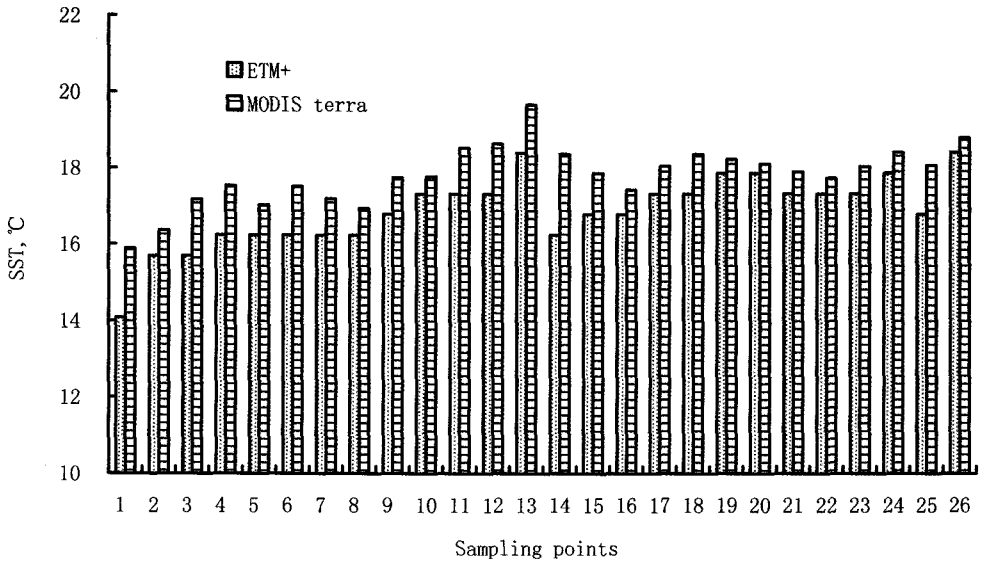

Fig. 6. The SST retrieved by ETM+ local algorithm vs. SST retrieved by MODIS terra split-window algorithm.

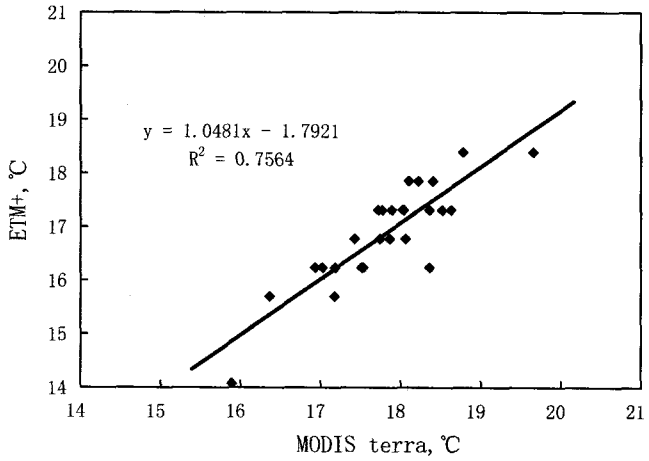

Fig. 7. The relationship between the SST retrieved by ETM+ local algorithm and MODIS terra split-window algorithm.

in this field (Wilson and Anderson 1984; Mustard *et al.* 1991; Tang *et al.* 2003). In recent years, the cooling water discharge from nuclear power plants is of concern (Chen *et al.* 2003; Ahn *et al.* 2006).

Based on the local algorithm introduced above, three Landsat TIR images acquired at different time are processed, and the results of SST are shown in Fig. 8. As shown in Fig. 8a which was acquired before the operation of Daya Bay Nuclear Power Station (DNPS), no obvious SST gradient was observed; and in the next two images acquired after the operation of DNPS, the thermal plume could be detected clearly. In Daya Bay, the mean SST is at the lowest in winter and spring (Qu *et al.* 2006); as shown in Fig. 8b and Fig. 8c, the strong vertical mixing of sea water will lead to a larger SST gradient, and a relatively smaller area of the thermal plume which even cannot be detected by AVHRR (Tang *et al.* 2003). In summer and autumn, the mean SST is at the highest, and water stratification often happens to Daya Bay; thermal effluent will increase this phenomenon. The summer distribution pattern of thermal plume can also be monitored and quantified through Landsat-5 TIR image (Chen *et al.* 2003). The information about the fine structure of thermal plume detected from Landsat data can be used to validate the forecasting accuracy of hydrodynamic model (Zeng *et al.* 2002), to which the AVHRR or MODIS SST products cannot be comparable due to their coarse spatial resolution of 1.1 km.

4. Conclusions and Perspectives

A useful method was developed to convert the TIR radiance between Landsat-7 and Landsat-5 as: $L_{\lambda,L5/TM}=0.9699\times L_{\lambda,L7/ETM+}+0.1074$ ($R^2=1$), and DN value can be converted accordingly. Via this converting method, it is easy to integrate the data of Landsat-7 and Landsat-5 to retrieve SST on the basis of local empirical algorithm in which the radiance or DN of Landsat-5 and 7 TIR band is usually the only input independent variable.

The result of validation work conducted in Daya Bay implied that the integrating method was effective, and the

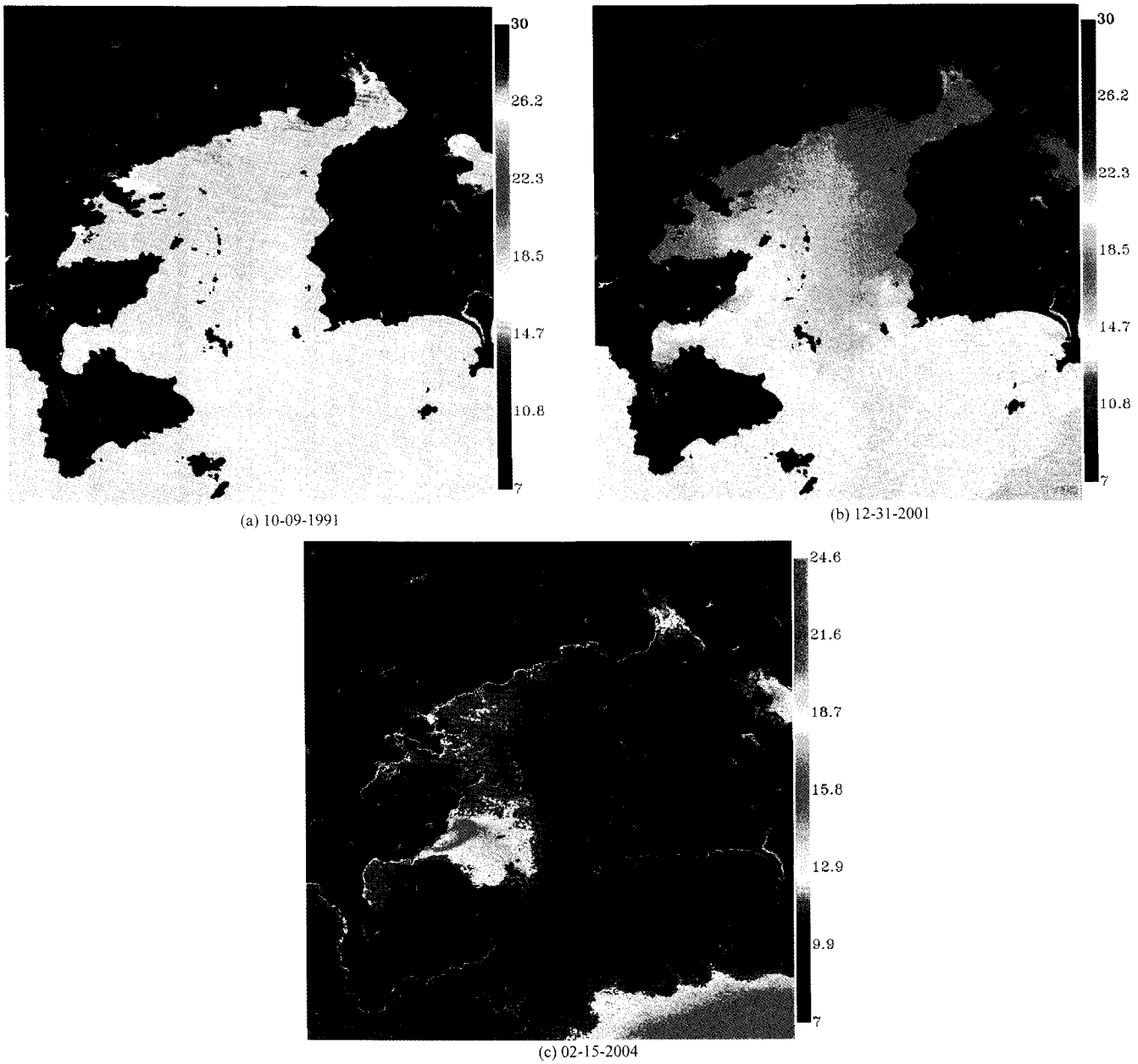

Fig. 8. The SST distribution of Daya Bay before and after the operation of DNPS (Unit, °C).

accuracy of SST retrieval was satisfying. This integrating method was further applied in Daya Bay to retrieve SST and monitor the thermal pollution of cooling water discharged from DNPS. The results of application work indicate that the TIR remote sensing technique could provide fine distribution pattern of thermal pollution when high spatial resolution TIR data are applied, and it is a useful tool for monitoring the environmental change of coastal waters.

Acknowledgements

This work was supported by "973" Program of China under contract No. 2001CB409708, "863" Program of China under contract No. 2002AA639130, and the Science and Technology Innovation Program of Guangdong Province, China under contract No. 2KB06701S. The authors are grateful to China Remote Sensing Satellite Ground Station and Global Land Cover Facility, University of Maryland for

the provided TM and ETM+ data.

References

Ahn, Y., P. Shanmugam, J. Lee, and Y.Q. Kang. 2006. Application of satellite infrared data for mapping of thermal plume contamination in coastal ecosystem of Korea. *Mar. Environ. Res.*, **61**(2), 186-201.

Chander, G. and B. Markham. 2003. Revised Landsat-5 TM radiometric calibration procedures and postcalibration dynamic ranges. *IEEE T. Geosci. Remote Sens.*, **41**(11), 2674-2677.

Chen, C., P. Shi, and Q. Mao. 2003. Application of remote sensing techniques for monitoring the thermal pollution of cooling-water discharge from nuclear power plant. *J. Environ. Sci. Heal. A*, **A38**(8), 1659-1668.

Chen, X., Y.S. Li, Z. Liu, K. Yin, Z. Li, O.W. Wai, and B. King. 2004. Integration of multi-source data for water quality classification in the Pearl River estuary and its adjacent coastal waters of Hong Kong. *Cont. Shelf Res.*, **24**(16), 1827-1843.

Gibbons, D.E., G.E. Wukelic, J.P. Leighton, and M.J. Doyle. 1989. Application of Landsat thematic mapper data for coastal thermal plume analysis at Diablo Canyon. *Photogramm. Eng. Rem. Sens.*, **55**(6), 903-909.

Landsat Project Science Office. 2006. Landsat 7 Science Data User's Handbook. Available from WWW: <http://ltpwww.gsfc.nasa.gov/IAS/handbook/handbook_toc.html>[cited: 2006-02-26].

Mustard, J.F., M.A. Carney, and A. Sen. 1999. The use of satellite data to quantify thermal effluent impacts. *Estur. Coast. Shelf S.*, **49**(4), 509-524.

Qin, Z, A. Karnieli, and P. Berliner. 2001. A mono-window algorithm for retrieving land surface temperature from Landsat TM data and its application to the Israel–Egypt border region. *Int. J. Remote Sens.*, **22**(18), 3719-3746.

Qu, M., Q. Xing, and W. Pan. 2006. The parameters of assessing Daya Bay water quality by remote sensing. *Ecologic Sci.* (In press) (In Chinese)

Ritchie, J.C. and C.M. Cooper. 2001. Remote sensing techniques for determining water quality: Application to TMDLs. p. 367-374. In: *TMDL Science Issues Conference*, Water Environment Federation, Alexandria, VA.

Suga, Y., H. Ogawa, K. Ohno, and K. Yamada 2003. Detection of surface temperature from Landsat-7/ETM+. *Adv. Space Res.*, **32**(11), 2235-2240.

Schott, J.R. 1982. An application of heat capacity mapping mission data: thermal bar studies of Lake Ontario. *J. Appl. Photogr. Eng.*, **8**(3), 117-120.

Schott, J.R., J.A. Barsi, B.L. Nordgren, N.G. Raqueño, and D. de Alwis. 2001. Calibration of Landsat thermal data and application to water resource studies. *Remote Sens. Environ.*, **78**(1-2), 108-117.

Tang, D.L., D.R. Kester, Z. Wang, J. Lian, and H. Kawamura. 2003. AVHRR satellite remote sensing and shipboard measurements of the thermal plume from the Daya Bay, nuclear power station, China. *Remote Sens. Environ.*, **84**(4), 506-515.

Thomas, A., D. Byrne, and R. Weatherbee. 2002. Coastal sea surface temperature variability from Landsat infrared data. *Remote Sens. Environ.*, **81**(2-3), 262-272.

Vogelmann, J.E., D. Helder, R. Morfitt, M.J. Choate, J.W. Merchant, and H. Bulley. 2001. Effects of Landsat 5 Thematic Mapper and Landsat 7 Enhanced Thematic Mapper Plus radiometric and geometric calibrations and corrections on landscape characterization. *Remote Sens. Environ.*, **78**(1-2), 55-70.

Weng, Q., D. Lu, and J. Schubring. 2004. Estimation of land surface temperature–vegetation abundance relationship for urban heat island studies. *Remote Sens. Environ.*, **89**(4), 467-483.

Wilson, S. B. and J.M. Anderson. 1984. A thermal plume in the Tay Estuary detected by aerial thermography. *Int. J. Remote Sens.*, **5**(1), 247-249.

Xing, Q., C. Chen, P. Shi, J. Yang, and S. Tang. 2006. Atmospheric correction of Landsat data for the retrieval of sea surface temperature in coastal waters. *Acta Oceanologia Sinica*, 25(3). (In press)

Xu, G. 1989. The environment and resources in daya bay: part I the environment of daya bay waters. Anhui Science and Technology Press, Hefei, Anhui, China. 108 p. (In Chinese)

Zeng, P., H. Chen, B. Ao, P. Ji, X. Wang, and Z. Ou. 2002. Transport of waste heat from a nuclear power plant into coastal water. *Coast. Eng.*, **44**(4), 301-319.